

Combined study of $b \rightarrow s\gamma$ and the muon anomalous magnetic moment in gauge-mediated supersymmetry breaking modelsK. T. Mahanthappa^{1*} and Sechul Oh^{2†}¹ *Department of Physics, University of Colorado, Boulder, Colorado 80309, USA*² *Institute of Physics and Applied Physics, Yonsei University, Seoul, 120-749, Korea*
(August, 1999)**Abstract**

We study both the branching ratio for $b \rightarrow s\gamma$ decay and the muon anomalous magnetic moment, $a_\mu \equiv (g - 2)_\mu/2$, in the minimal supersymmetric standard model with gauge-mediated supersymmetry breaking. Combining new experimental data on a_μ and the branching ratio for $b \rightarrow s\gamma$, strong limits on the parameter space of these models are derived. We find that this combined study leads to much stronger constraints on the parameter space of the model than those from either $b \rightarrow s\gamma$ or a_μ . In particular, the region of large $\tan\beta$ is extremely limited, which would have been otherwise allowed. We include the supersymmetric one-loop correction to the mass of b quark, m_b , and find that in order to have a correct value of m_b , the region of large $\tan\beta$ and $\mu < 0$ (in our convention) is not allowed in these models. The region of large $\tan\beta$ and $\mu > 0$ is also strongly constrained. We present bounds on supersymmetric particle masses as a function of $\tan\beta$.

^{*}ktm@verb.colorado.edu[†]scoh@kimcs.yonsei.ac.kr

Supersymmetry (SUSY) is a very attractive candidate beyond the standard model (SM) since it provides an elegant solution to the hierarchy problem in particle physics. Understanding the mechanism of SUSY breaking and its communication to the observable sector is one of the most important open questions. There are two types of realistic supersymmetric models of interest : gravity-mediated models and models with gauge-mediated SUSY breaking (GMSB). The GMSB models [1] have been of special interest, because they have attractive features of natural suppression of the SUSY contributions to flavor-changing neutral currents at low energies and prediction of the supersymmetric particle mass spectrum in terms of few parameters.

The parameters of SUSY models can be constrained by using precision measurements in low energy experiments, because superparticles contribute to low energy physics through radiative corrections. In particular, experimentally observed rare decays may shed light on the parameter space of SUSY models. Processes such as $b \rightarrow s\gamma$ do not occur at the tree level, and at one-loop level they occur at a small rate but enough to be sensitive to new physics effects [2]. The CLEO collaboration has recently reported the branching ratio for the decay $b \rightarrow s\gamma$ [3] : $\text{BR}(b \rightarrow s\gamma) = (3.15 \pm 0.35 \pm 0.32 \pm 0.26) \times 10^{-4}$, which corresponds to the bound $2.0 \times 10^{-4} < \text{BR}(b \rightarrow s\gamma) < 4.5 \times 10^{-4}$ at 95 % C.L. The anomalous magnetic moment of muon, $a_\mu \equiv (g - 2)_\mu/2$, is also sensitive to new physics effects and can be used to constrain SUSY models [4–6], on account of the great accuracy of both experimental and SM theoretical values of a_μ . The present experimental value of a_μ [7] is $a_\mu^{\text{exp}} = 11659230(84) \times 10^{-10}$, while the theoretical prediction for a_μ in the context of the SM [8,9] is $a_\mu^{\text{SM}} = 11659162(6.5) \times 10^{-10}$.

In this paper, we obtain combined constraints due to both $b \rightarrow s\gamma$ decay and a_μ in the minimal supersymmetric SM (MSSM) with GMSB. Even though there exist the previous works which studied either $b \rightarrow s\gamma$ [10,11] or a_μ [6] in the GMSB models, our work extends the previous ones in the sense that we investigate both $b \rightarrow s\gamma$ and a_μ together with the inclusion of the supersymmetric one-loop correction to the mass of b quark, m_b , which has considerable effects in large $\tan\beta$ region [12,13]. We shall see that this combined study leads to much stronger constraints on the parameter space of the model than those from either $b \rightarrow s\gamma$ or a_μ . In particular, the region of large $\tan\beta$ is extremely limited, which would have been otherwise allowed. Furthermore, in this work, we explicitly show that, with the presently available experimental data, constraints from the decay $b \rightarrow s\gamma$ are more stringent than those from a_μ in broad region of the parameter space. We also present bounds on supersymmetric particle masses as a function of $\tan\beta$.

In the GMSB models messenger fields transmit SUSY breaking to the fields of visible sector via loop diagrams involving $\text{SU}(3)_C \times \text{SU}(2)_L \times \text{U}(1)_Y$ gauge interactions. The simplest model consists of messenger fields which transform as a single flavor of vectorlike $\mathbf{5} + \bar{\mathbf{5}}$ of $\text{SU}(5)$. These messenger fields may be coupled to a SM singlet chiral superfield S through the superpotential

$$W_{\text{messenger}} = \lambda_D S D \bar{D} + \lambda_L S L \bar{L}, \quad (1)$$

where the fields have the SM representations and quantum numbers $D : (\mathbf{3}, \mathbf{1})_{Y=-2/3}$, $\bar{D} : (\bar{\mathbf{3}}, \mathbf{1})_{Y=2/3}$, $L : (\mathbf{1}, \mathbf{2})_{Y=-1}$, and $\bar{L} : (\mathbf{1}, \mathbf{2})_{Y=1}$. The scalar and F components of S acquire VEVs $\langle S \rangle$ and $\langle F_S \rangle$, respectively, through their interactions with the fields of hidden sector, which results in breakdown of SUSY. It is known that for messenger fields in complete $\text{SU}(5)$

representation, at most four $(\mathbf{5}+\bar{\mathbf{5}})$ pairs, or one $(\mathbf{5}+\bar{\mathbf{5}})$ and one $(\mathbf{10}+\bar{\mathbf{10}})$ pair are allowed to ensure that the gauge couplings remain perturbative up to the grand unified theory (GUT) scale [14].

In general, the parameters μ and B in soft SUSY breaking terms depend on the details of the SUSY breaking in the hidden sector. We require that electroweak symmetry be radiatively broken, which determines μ^2 and B in terms of other parameters of the theory. Then the sparticle masses depend on five independent parameters: M , Λ , n , $\tan\beta$, and $\text{sign}(\mu)$. Here M is the messenger scale given by $M = \lambda \langle S \rangle$ with a universal Yukawa coupling λ in the messenger sector at GUT scale. The parameter Λ is defined by $\Lambda = \langle F_S \rangle / \langle S \rangle$. The integer number n is the effective number of messenger fields given by $n = n_5 + 3n_{10}$, where n_5 and n_{10} denote the number of $(\mathbf{5}+\bar{\mathbf{5}})$ and $(\mathbf{10}+\bar{\mathbf{10}})$ pairs, respectively. The radiatively generated soft SUSY-breaking masses of gaugino and scalars, \tilde{M}_i and \tilde{m}^2 , at messenger scale M are given by [15,16]

$$\tilde{M}_i(M) = ng(x) \frac{\alpha_i(M)}{4\pi} \Lambda, \quad (2)$$

$$\tilde{m}^2(M) = 2nf(x) \sum_{i=1}^3 k_i C_i \left(\frac{\alpha_i(M)}{4\pi} \right)^2 \Lambda^2, \quad (3)$$

where $x \equiv \Lambda/M$. α_i ($i = 1, 2, 3$) are the three SM gauge couplings with GUT normalization for α_1 . k_i are 1, 1, 3/5 for $\text{SU}(3)_C$, $\text{SU}(2)_L$ and $\text{U}(1)_Y$, respectively. C_i are zero for gauge singlets, and 4/3, 3/4 and $(Y/2)^2$ for the fundamental representations of $\text{SU}(3)_C$, $\text{SU}(2)_L$ and $\text{U}(1)_Y$, respectively (with Y defined by $Q = I_3 + Y/2$). $g(x)$ and $f(x)$ are messenger scale threshold functions.

We use the input values $\alpha_s(M_Z) = 0.118$, $\sin^2 \theta_W(M_Z) = 0.2315$ and $\alpha(M_Z) = 1/128$. The parameter Λ is taken to be around 100 TeV to ensure that the sparticle masses are of the order of the weak scale. We restrict $1 < M/\Lambda < 10^4$: the case $M = \Lambda$ is excluded since it produces a massless scalar in the messenger sector [15,16] and the upper bound on the gravitino mass of about 10^4 eV restricts $M/\Lambda < 10^4$ [16,17]. Using the appropriate renormalization group equations (RGEs) [18], we first go up to the messenger scale M with gauge and Yukawa couplings, and fix the sparticle masses with the boundary conditions (2) and (3). We next go down with the 6×6 mass matrices for the squarks and sleptons to find the sparticle spectrum. In running the RGEs, we include the one-loop correction to the running bottom quark mass, Δm_b , which involves the contributions coming from gluino–bottom-squark loop diagram and chargino–top-squark loop diagram, and is given by [12]

$$\Delta m_b = -\lambda_b v_1 \mu \tan \beta \left[\frac{2\alpha_s}{3\pi} M_{\tilde{g}} I(m_{\tilde{b}_1}^2, m_{\tilde{b}_2}^2, M_{\tilde{g}}^2) + \frac{\lambda_t^2}{(4\pi)^2} A_t I(m_{\tilde{t}_1}^2, m_{\tilde{t}_2}^2, \mu^2) \right], \quad (4)$$

where the integral function $I(a, b, c)$ is given by

$$I(a, b, c) = -\frac{ab \ln(a/b) + bc \ln(b/c) + ca \ln(c/a)}{(a-b)(b-c)(c-a)}, \quad (5)$$

and $M_{\tilde{g}}$ is the gluino mass and $m_{\tilde{b}_i}$ ($m_{\tilde{t}_i}$) is the bottom-squark (top-squark) eigenstate masses, respectively. Our convention for the sign of the Higgs boson mass parameter μ follows that in Ref. [18].

Calculation of $b \rightarrow s\gamma$ amplitude involves the coefficients of short distance photonic and gluonic operators $c_7(M_W)$ and $c_8(M_W)$. The SM calculations of c_7 and c_8 with QCD corrections to two-loop order are given in Ref. [19]. Calculations of next-to-leading order agree with the previous calculations while reducing the theoretical errors [20]. Various supersymmetric contributions for $b \rightarrow s\gamma$ are given in a generic form in Ref. [21]. The branching ratio for $b \rightarrow s\gamma$ is given by [22]

$$\text{BR}(b \rightarrow s\gamma) = \frac{6\alpha [\eta^{16/23} A_\gamma + \frac{8}{3}(\eta^{14/23} - \eta^{16/23}) A_g + C]^2}{\pi I(m_c/m_b)[1 - \frac{2}{3\pi}\alpha_s(m_b)f(m_c/m_b)]} \text{BR}(b \rightarrow ce\bar{\nu}), \quad (6)$$

where $\eta = \alpha_s(M_Z)/\alpha_s(m_b)$. I is the phase-space factor given by $I(x) = 1 - 8x^2 + 8x^6 - x^8 - 24x^4 \ln x$, and f is the QCD correction factor for the semileptonic decay given by $f(m_c/m_b) = 2.41$. A_γ and A_g are the coefficients of the effective $bs\gamma$ and bsg penguin operators evaluated at the scale M_Z , respectively. $\text{BR}(b \rightarrow ce\bar{\nu})$ denote the branching ratio of the semileptonic decay $b \rightarrow ce\bar{\nu}$.

The supersymmetric contributions to the muon anomalous magnetic moment a_μ are essentially coming from neutralino($\tilde{\chi}^0$)-smuon($\tilde{\mu}$) loop diagram and chargino($\tilde{\chi}^\pm$)-sneutrino($\tilde{\nu}$) loop diagram as follows [5,6] :

$$\delta a_\mu^{\text{SUSY}} = \delta a_\mu^{\text{N}} + \delta a_\mu^{\text{C}}. \quad (7)$$

Here δa_μ^{N} and δa_μ^{C} denote the contributions from the $\tilde{\chi}^0$ - $\tilde{\mu}$ diagram and $\tilde{\chi}^\pm$ - $\tilde{\nu}$ diagram, respectively, and are given by

$$\begin{aligned} \delta a_\mu^{\text{N}} = & \frac{m_\mu}{16\pi^2} \sum_{i,\alpha} \left[-\frac{m_\mu}{6m_{\tilde{\mu}_i}^2(1-x_{i\alpha})^4} (N_{i\alpha}^L N_{i\alpha}^L + N_{i\alpha}^R N_{i\alpha}^R) (1 - 6x_{i\alpha} + 3x_{i\alpha}^2 + 2x_{i\alpha}^3 - 6x_{i\alpha}^2 \ln x_{i\alpha}) \right. \\ & \left. - \frac{m_{\tilde{\chi}_\alpha^0}}{m_{\tilde{\mu}_i}^2(1-x_{i\alpha})^3} N_{i\alpha}^L N_{i\alpha}^R (1 - x_{i\alpha}^2 + 2x_{i\alpha} \ln x_{i\alpha}) \right], \end{aligned} \quad (8)$$

$$\begin{aligned} \delta a_\mu^{\text{C}} = & \frac{m_\mu}{16\pi^2} \sum_l \left[\frac{m_\mu}{3m_{\tilde{\nu}}^2(1-x_l)^4} (C_l^L C_l^L + C_l^R C_l^R) \left(1 - \frac{3}{2}x_l - 3x_l^2 + \frac{1}{2}x_l^3 + 3x_l \ln x_l \right) \right. \\ & \left. - \frac{3m_{\tilde{\chi}_l^\pm}}{m_{\tilde{\nu}}^2(1-x_l)^3} C_l^L C_l^R \left(1 - \frac{4}{3}x_l + \frac{1}{3}x_l^2 + \frac{2}{3} \ln x_l \right) \right], \end{aligned} \quad (9)$$

where $(i, l = 1, 2; \alpha = 1 - 4)$

$$\begin{aligned} x_{i\alpha} &= m_{\tilde{\chi}_\alpha^0}^2/m_{\tilde{\mu}_i}^2, \quad x_l = m_{\tilde{\chi}_l^\pm}^2/m_{\tilde{\nu}}^2, \\ N_{i\alpha}^L &= -\frac{m_\mu}{v_1} (U^N)_{3\alpha} (U^{\tilde{\mu}})_{Li} + \sqrt{2} g_Y (U^N)_{1\alpha} (U^{\tilde{\mu}})_{Ri}, \\ N_{i\alpha}^R &= -\frac{m_\mu}{v_1} (U^N)_{3\alpha} (U^{\tilde{\mu}})_{Ri} - \frac{g_2}{\sqrt{2}} (U^N)_{2\alpha} (U^{\tilde{\mu}})_{Li} - \frac{g_Y}{\sqrt{2}} (U^N)_{1\alpha} (U^{\tilde{\mu}})_{Li}, \\ C_l^L &= \frac{m_\mu}{v_1} (U^C)_{l2}, \quad C_L^R = -g_2 (V^C)_{l1}. \end{aligned} \quad (10)$$

g_2 and g_Y are the gauge couplings of $SU(2)_L$ and $U(1)_Y$, respectively, and v_1 is the vacuum expectation value of the Higgs boson H_1 . m_μ , $m_{\tilde{\chi}^0}$, $m_{\tilde{\chi}^\pm}$, $m_{\tilde{\mu}}$, and $m_{\tilde{\nu}}$ are masses of the muon, neutralino, chargino, smuon, and sneutrino, respectively. U^N and $U_{L,R}^{\tilde{\mu}}$ denote the neutralino and smuon mixing matrices, and U^C and V^C denote the chargino mixing matrices.

We use our calculated mass spectrum and couplings to calculate the rate for $b \rightarrow s\gamma$ and $\delta a_\mu^{\text{SUSY}}$. For fixed values of $\tan\beta$, n and $\text{sgn}(\mu)$, both the branching ratio for $b \rightarrow s\gamma$ and $\delta a_\mu^{\text{SUSY}}$ as well as $|\mu|$ and the weak gaugino mass M_2 are calculated, as the values of M and Λ vary. Then the bounds on the branching ratio for $b \rightarrow s\gamma$ and $\delta a_\mu^{\text{SUSY}}$ are translated into the bounds on values of M_2 and $|\mu|$ in the $|\mu| - M_2$ plane for fixed values of $\tan\beta$, n and $\text{sgn}(\mu)$. From Eq. (2) one can see that M_2 is directly related to Λ , since $g(x) \simeq 1$. Bounds on other sparticle masses can be easily deduced from a bound on M_2 , owing to the relations Eqs. (2) and (3).

In $b \rightarrow s\gamma$ decay, the contributions to the total decay amplitude are coming from the W loop diagram, charged Higgs boson loop diagram, neutralino loop diagram, and gluino loop diagram. It has been pointed out that the neutralino and gluino contributions to the amplitude are less than 1 % in the whole range of parameter space [11]. The charged Higgs boson loop contribution adds constructively to the W loop contribution, while the chargino loop contribution can be constructive or destructive to the W loop contribution, but is generally much smaller than the charged Higgs boson loop contribution. We use the new CLEO bound on the branching ratio for $b \rightarrow s\gamma$ decay in order to obtain constraints on the parameter space of the GMSB models.

The bound on the supersymmetric contributions to a_μ is given by $-71 \times 10^{-10} < \delta a_\mu^{\text{SUSY}} < 207 \times 10^{-10}$ at 90 % C.L. This bound is obtained by the difference between experimental value and theoretical prediction of a_μ . The new E821 experiment at Brookhaven is expected to improve the experimental determination of a_μ to the level of 4×10^{-10} [23]. Since the complete two-loop electroweak contribution in the SM to a_μ is $a_\mu^{\text{EW}} = 15.1(0.4) \times 10^{-10}$ [9] and the supersymmetric contributions can be as large or even larger than the a_μ^{EW} , it is expected that the new E821 experiment will be possible to test both the SM electroweak and supersymmetric contributions [4–6].

In Figs. 1–8, we display the bounds obtained from the branching ratio for $b \rightarrow s\gamma$ and $\delta a_\mu^{\text{SUSY}}$ in the $|\mu| - M_2$ plane for either sign of μ , for $\tan\beta = 10$ and 60, and for $n = 1$ and 3, respectively. Solid lines represent the bounds from the branching ratio for $b \rightarrow s\gamma$ and dot-dashed lines describe the bounds from $\delta a_\mu^{\text{SUSY}}$. Figures 1 and 2 show the bounds on M_2 and $|\mu|$ for $\tan\beta = 10$ and $n = 1$, and for positive and negative μ , respectively. The region surrounded by the solid line is allowed by the CLEO bound, while the upper region of the dot-dashed line is allowed by the present bound on a_μ . In the case of Fig. 1, the constraint from $b \rightarrow s\gamma$ decay is clearly much stronger than that from a_μ . We find $M_2 > 248$ GeV and $\mu > 626$ GeV. Small values of M_2 lead to unacceptably large contribution to the branching ratio for $b \rightarrow s\gamma$, while large values of μ raise the problem of fine-tuning and are generally constrained by the lower bound on the stau mass. In Fig. 2 we see the constraints from both $b \rightarrow s\gamma$ and a_μ are complementary. By combining the bounds from the both, we can obtain much stronger bound on M_2 and $|\mu|$; in particular, low values of $|\mu|$ which would have been allowed are excluded. We find $M_2 > 210$ GeV and $|\mu| > 505$ GeV.

In large $\tan\beta$ case, we find that the bound from either $b \rightarrow s\gamma$ or a_μ is more stringent than that in small $\tan\beta$ case, and most region in the $|\mu| - M_2$ plane is excluded. For

$\tan\beta = 60$ and $\mu > 0$ (Figs. 3 and 6), the allowed regions from each of $b \rightarrow s\gamma$ and a_μ do not overlap, even though a possibility exists that they might overlap for unacceptably very large values of μ . Thus, this case is excluded, while it would be allowed if one considered only either $b \rightarrow s\gamma$ or a_μ as in Refs. [6,11]. For $\tan\beta \lesssim 50$ and $\mu > 0$, the allowed regions from each of $b \rightarrow s\gamma$ and a_μ overlap allowing limited regions in the parameter space. For $\tan\beta = 60$ and $\mu < 0$, the supersymmetric one-loop correction to bottom quark mass leads to unacceptably large value of m_b . In other words, in order to have a correct value of m_b , the negative sign of μ is not physically allowed for large $\tan\beta$ in our analysis. It can be qualitatively understood from Eq. (4) : for large $\tan\beta$, the correction Δm_b is large, and for negative μ , Δm_b gives positive contribution leading to an incorrect value of m_b . Thus, by inclusion of the correction Δm_b , we exclude the case of large $\tan\beta$ and $\mu < 0$. This result is different from those in the previous works : in Ref. [11] the one-loop correction Δm_b was not taken into account and the case of large $\tan\beta$ and $\mu < 0$ was favored without any constraint from $b \rightarrow s\gamma$. Also, in Ref. [6], the case of large $\tan\beta$ and $\mu < 0$ is allowed with a constraint on the value of M_2 .

For $n = 3$, the constraints from each of $b \rightarrow s\gamma$ and a_μ are more stringent. But after combining the constraints together, we find that for $\tan\beta = 10$ and $\mu < 0$, the resulting limits are lower (i.e., $M_2 > 182$ GeV and $|\mu| > 320$ GeV) than those in the case of $n = 1$, while for $\tan\beta = 10$ and $\mu > 0$, the resulting limits are still higher (i.e., $M_2 > 357$ GeV and $\mu > 648$ GeV). For $n = 3$, large $\tan\beta$ region is almost ruled out due to the same reason as the case of $n = 1$.

In Figs. 7 and 8 we plot the bounds on the sparticle masses, obtained by this combined analysis of $b \rightarrow s\gamma$ and a_μ , as a function of $\tan\beta$ for positive μ and for $n = 1$ and 3, respectively. The plots are displayed for up to $\tan\beta \approx 50$, since the region corresponding to $\tan\beta \gtrsim 50$ is ruled out. The lower bounds on the sparticle masses increase monotonically as $\tan\beta$ does. For $n = 3$, the lower bound on each sparticle mass is higher than that for $n = 1$. (We show the plots in the positive μ case only, because for negative μ the allowed parameter space is restricted to only relatively small $\tan\beta$ region ($\tan\beta \lesssim 20$) in order to have a correct value of m_b in our analysis.)

Some comments concerning the non-leading order (NLO) corrections to $b \rightarrow s\gamma$ are in order. It has been pointed out by Kagan and Neubert [24] that NLO corrections lead to a 10% error in predicted theoretical values. Ciuchini *et al.* [25] find that, when the leading order (LO) corrections cancel, contributions from NLO corrections become significant; this happens when the masses of charginos and right-handed top-squark are very much higher than those of other squarks and the gluino. In our parametric space such a cancellation of LO corrections is unlikely. There could be other circumstances leading to the cancellation of LO corrections, and this is under investigation.

In conclusion, we have investigated both the $b \rightarrow s\gamma$ decay and the anomalous magnetic moment of muon a_μ together in MSSM with GMSB. We have used the new CLEO bound on the branching ratio for $b \rightarrow s\gamma$ and the present experimental limit on a_μ to constrain the parameter space of the GMSB models. We have presented bounds on supersymmetric particle masses as a function of $\tan\beta$. This combined study has led to much stronger constraints on the parameter space of the model than those from either $b \rightarrow s\gamma$ or a_μ . In particular, the region of large $\tan\beta$, which would have been otherwise allowed, is ruled out or severely constrained, depending on the sign of μ . With the inclusion of the supersymmetric one-loop

correction to b quark mass, we have found that the region of large $\tan\beta$ and negative μ is physically ruled out in order to give a correct value of m_b . The present experimental data on the decay $b \rightarrow s\gamma$ leads to more stringent constraints than those from a_μ in a broad region of the parameter space. The anticipated precision level of 4×10^{-10} in determination of a_μ in the Brookhaven E821 experiment would constrain the parameter space much more severely.

We thank Jim Smith and B. Dutta for helpful discussions. This work was supported in part by the US Department of Energy Grant No. DE FG03-95ER40894.

REFERENCES

- [1] M. Dine and A.E. Nelson, Phys. Rev. D **48**, 1277 (1993); M. Dine, A.E. Nelson, and Y. Shirman, *ibid.* **51**, 1362 (1995); M. Dine, A.E. Nelson, Y. Nir, and Y. Shirman, *ibid.* **53**, 2658 (1996); for a review and references, see G.F. Giudice and R. Rattazzi, Phys. Rep. **322**, 419 (1999); **322** 501 (1999).
- [2] For some recent works, see C.S. Kim and Y.G. Kim, Phys. Rev. D **61**, 054008 (2000); T. Goto, Y.-Y. Keum, T. Nihei, Y. Okada, and Y. Shimizu, Phys. Lett. B **460**, 333 (1999); D. Bowser-Chao, K. Cheung, and W.-Y. Keung, Phys. Rev. D **59**, 115006 (1999); Y.G. Kim, P. Ko, and J.S. Lee, Nucl. Phys. **B544**, 64 (1999); C.-K. Chua, X.-G. He, and W.-S. Hou, Phys. Rev. D **60**, 014003 (1999); A.L. Kagan and M. Neubert, *ibid.* **58**, 094012 (1998); S.K. Biswas and V.P. Gautam, Hadronic J. **21**, 431 (1998); G. Barenboim, Nucl. Phys. **B534**, 318 (1998).
- [3] CLEO collaboration, S. Ahmed *et al.*, CLEO CONF 99-10, hep-ex/9908022, 1999.
- [4] P. Fayet, Phys. Lett. **70B**, 461 (1977); R. Barbieri and L. Maiani, *ibid.* **117B**, 203 (1982); J.A. Grifols and A. Mendez, Phys. Rev. D **26**, 1809 (1982); J. Ellis, J.S. Hagelin, and D.V. Nanopoulos, Phys. Lett. **116B**, 283 (1982); D.A. Kosower, L.M. Krauss, and N. Sakai, *ibid.* **133B**, 305 (1983); T.C. Yuan, R. Arnowitt, A.H. Chamseddine, and P. Nath, Z. Phys. C **26**, 407 (1984); J. Lopez, D.V. Nanopoulos, and X. Wang, Phys. Rev. D **49**, 366 (1994); U. Chattopadhyay and P. Nath, *ibid.* **53**, 1648 (1996); T. Ibrahim and P. Nath, *ibid.* (to be published) hep-ph/9907555; *ibid.* (to be published) hep-ph/9908443.
- [5] T. Moroi, Phys. Rev. D **53**, 6565 (1996); **56**, 4424(E) (1997); I. Vendramin, Nuovo Cimento A **101**, 731 (1989).
- [6] M. Carena, G.F. Giudice, and C.E.M. Wagner, Phys. Lett. B **390**, 234 (1997).
- [7] Particle Data Group, C. Caso *et al.*, Eur. Phys. J. C **3**, 280 (1998).
- [8] T. Kinoshita and W.J. Marciano, in *Quantum Electrodynamics*, edited by T. Kinoshita (World Scientific, Singapore, 1990); M. Davier and A. Hocker, Phys. Lett. B **419**, 419 (1998); M. Hayakawa and T. Kinoshita, Phys. Rev. D **57**, 465 (1998); J. Bijnens, E. Pallante, and J. Prades, Nucl. Phys. **B474**, 379 (1996).
- [9] A. Czarnecki, B. Krause, and W. Marciano, Phys. Rev. Lett. **76**, 3267 (1996); G. Degrossi and G.F. Giudice, Phys. Rev. D **58**, 053007 (1998).
- [10] S. Dimopoulos, S. Thomas, and J.D. Wells, Nucl. Phys. **B488**, 39 (1997); H. Baer, M. Brhlik, C.-H. Chen, and X. Tata, Phys. Rev. D **55**, 4463 (1997); J. Erler and D.M. Pierce, Nucl. Phys. **B526**, 53 (1998); H. Hamidian, K. Huitu, K. Puolamäki, and D.-X. Zhang, Phys. Lett. B **448**, 234 (1999); R. Rattazzi and U. Sarid, Nucl. Phys. **B501**, 297 (1997).
- [11] N.G. Deshpande, B. Dutta, and Sechul Oh, Phys. Rev. D **56**, 519 (1997).
- [12] R. Rattazzi and U. Sarid, Phys. Rev. D **53**, 1553 (1996); M. Carena, M. Olechowski, S. Pokorski, and C.E.M. Wagner, Nucl. Phys. **B426**, 269 (1994); K.S. Babu, B. Dutta, and R.N. Mohapatra, Phys. Lett. B **458**, 93 (1999).
- [13] T. Banks, Nucl. Phys. **B303**, 172 (1988); L.J. Hall, R. Rattazzi, and U. Sarid, Phys. Rev. D **50**, 7048 (1994).
- [14] T. Moroi, H. Murayama, and T. Yanagida, Phys. Rev. D **48**, 2995 (1993); B. Brahmachari, U. Sarkar, and K. Sridhar, Mod. Phys. Lett. A **8**, 3349 (1993).
- [15] S. Dimopoulos, S. Thomas, and J.D. Wells, Nucl. Phys. **B488**, 39 (1997); S.P. Martin, Phys. Rev. D **55**, 3177 (1997).

- [16] J.A. Bagger, K.T. Matchev, D.M. Pierce, and R.-J. Zhang, Phys. Rev. D **55**, 3188 (1997).
- [17] H. Pagels and J.R. Primack, Phys. Rev. Lett. **48**, 223 (1982); T. Moroi, H. Murayama, and M. Yamaguchi, Phys. Lett. B **303**, 289 (1993).
- [18] V. Barger, M. Berger, P. Ohmann, and R.J.N. Phillips, Phys. Rev. D **51**, 2438 (1995) and references therein.
- [19] T. Inami and C.S. Lim, Prog. Theor. Phys. **65**, 297 (1981); N.G. Deshpande and G. Eilam, Phys. Rev. D **26**, 2463 (1982).
- [20] C. Greub, T. Hurth, and D. Wyler, Phys. Lett. B **380**, 385 (1996); Phys. Rev. D **54**, 3350 (1996); J.L. Hewett and J.D. Wells, *ibid.* **55**, 5549 (1997).
- [21] S. Bertolini, F. Borzumati, A. Masiero, and G. Ridolfi, Nucl. Phys. **B353**, 591 (1991).
- [22] R. Barbieri and G. Giudice, Phys. Lett. B **309**, 86 (1993).
- [23] R.M. Carey *et al.*, Phys. Rev. Lett. **82**, 1632 (1999).
- [24] A.L. Kagan and M. Neubert, Eur. Phys. J. C **7**, 5 (1999).
- [25] M. Ciuchini, G. Degrandi, P. Gambino, and G.F. Giudice, Nucl. Phys. **B534**, 3 (1998).

FIGURE CAPTIONS

- Fig. 1 : Limits on the weak gaugino mass M_2 vs $|\mu|$ for $\tan\beta = 10$, $\mu > 0$ and $n = 1$. Units are in GeV. The solid line represents the bound from the branching ratio for $b \rightarrow s\gamma$ (the region surrounded by the solid line is allowed) and the dot-dashed line represents the lower bound from a_μ . Note that M_2 and $|\mu|$ are calculated and not independent. The value of M_2 increases as the value of $|\mu|$ increases in the allowed region.
- Fig. 2 : The same as Fig. 1, except $\mu < 0$.
- Fig. 3 : Limits on the weak gaugino mass M_2 vs μ for $\tan\beta = 60$, $\mu > 0$ and $n = 1$. Units are in GeV. The solid line represents the bound from the branching ratio for $b \rightarrow s\gamma$ (the region surrounded by the solid line is allowed) and the dot-dashed line represents the lower bound from a_μ . Note that M_2 and $|\mu|$ are calculated and not independent. The value of M_2 increases as the value of $|\mu|$ increases in the allowed region.
- Fig. 4 : The same as Fig. 1, except $n = 3$.
- Fig. 5 : The same as Fig. 2, except $n = 3$.
- Fig. 6 : The same as Fig. 3, except $n = 3$.
- Fig. 7 : Bounds on the sparticle masses (in GeV) as a function of $\tan\beta$ for $\mu > 0$ and $n = 1$. The solid line represents the lower bound on the gluino mass, and the dotted and dot-dashed lines represent the lower bounds on the stop ($m_{\tilde{t}_1}$ and $m_{\tilde{t}_2}$) and sbottom ($m_{\tilde{b}_1}$ and $m_{\tilde{b}_2}$) masses, respectively.
- Fig. 8 : The same as Fig. 7, except $n = 3$.

FIGURES

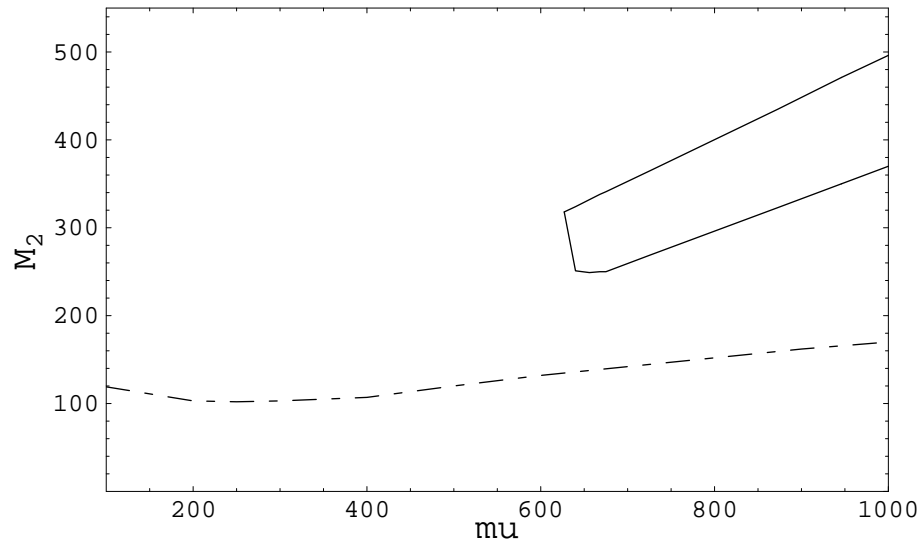


FIG. 1.

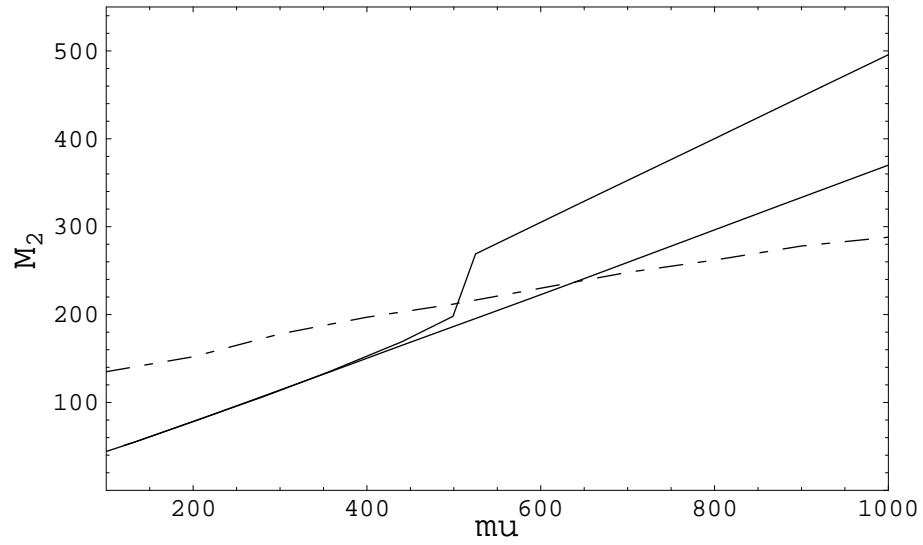


FIG. 2.

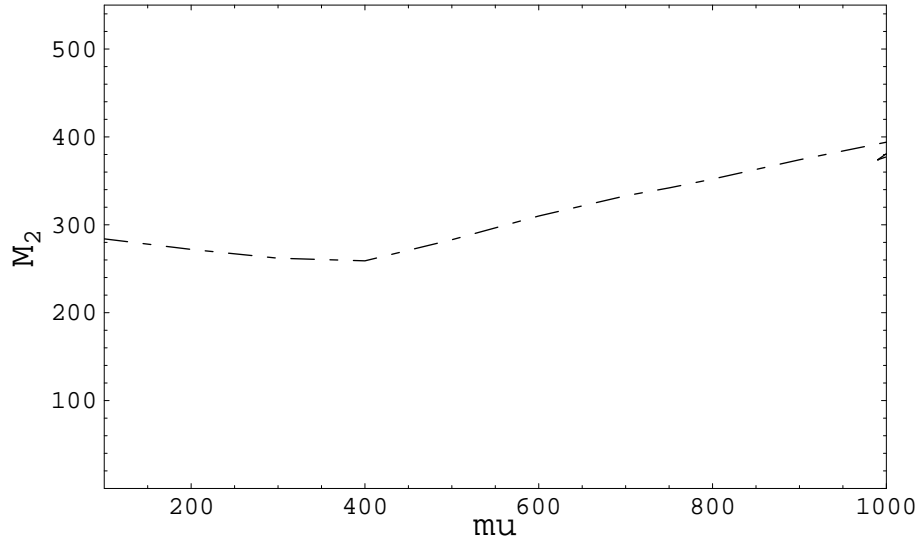


FIG. 3.

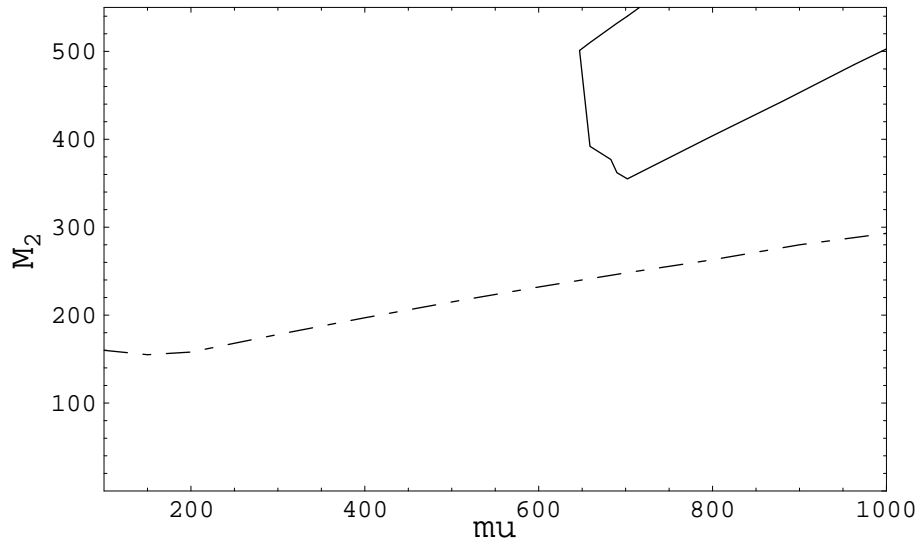


FIG. 4.

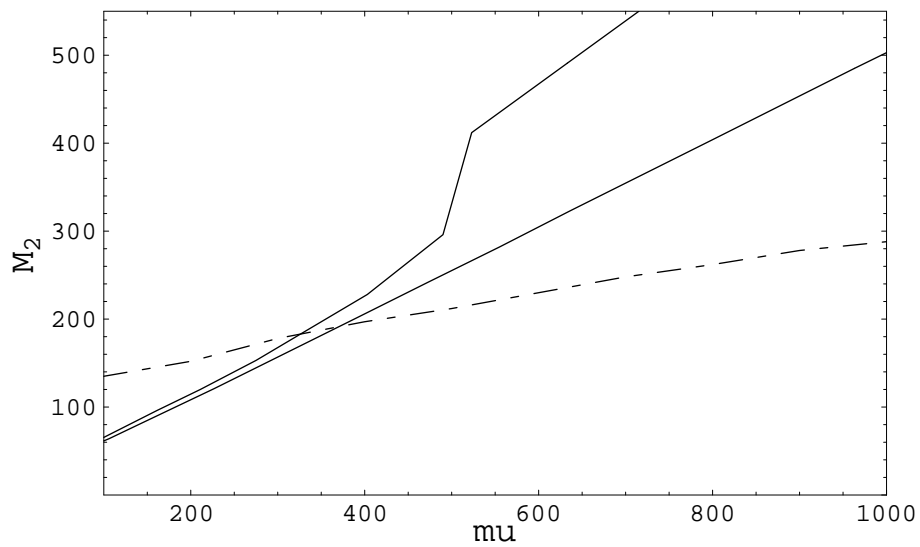


FIG. 5.

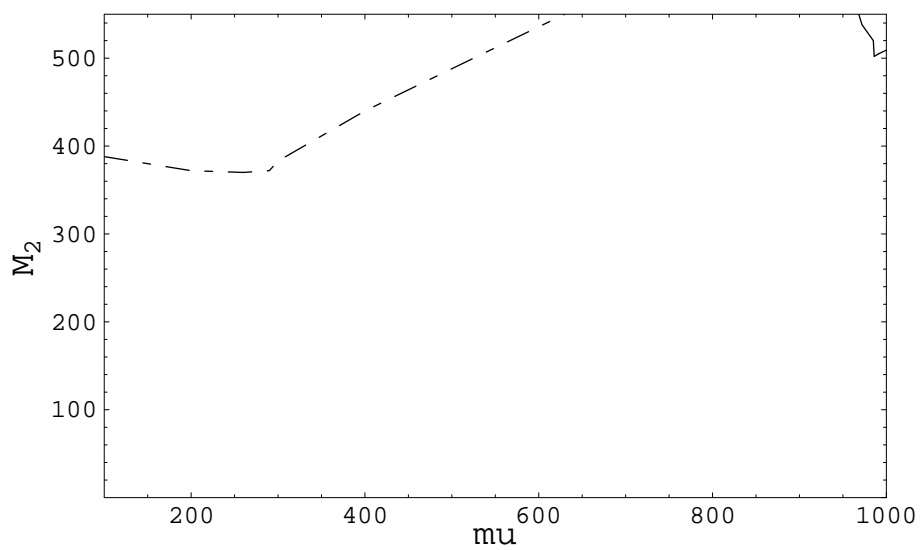


FIG. 6.

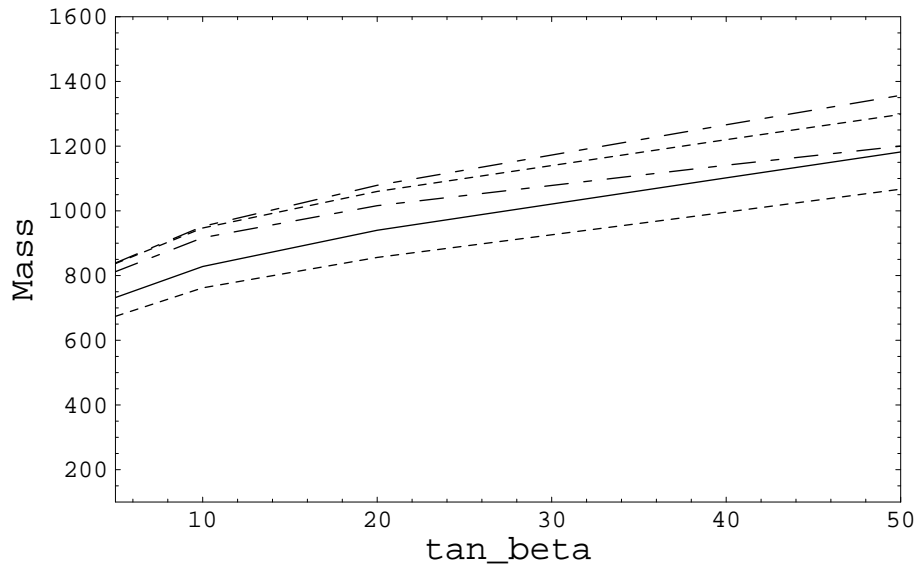


FIG. 7.

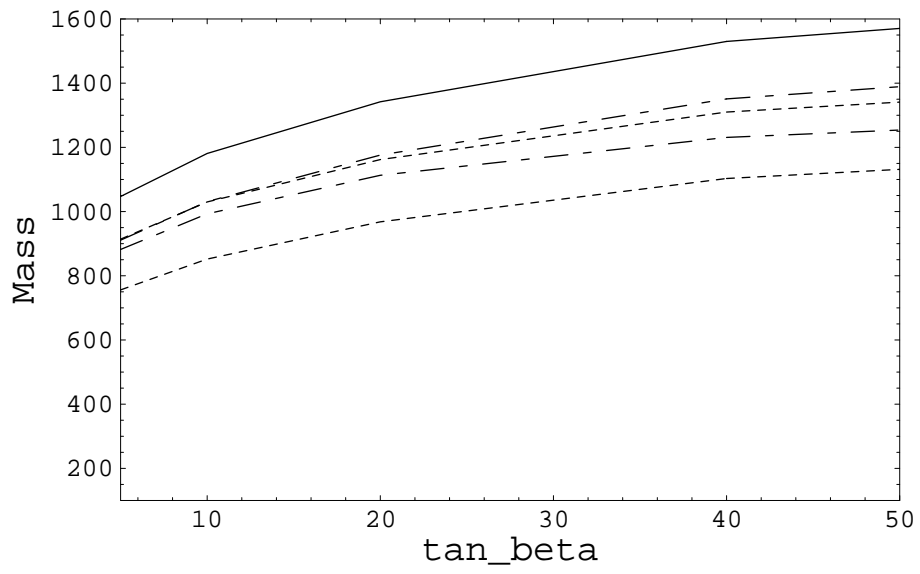


FIG. 8.